Journal of the European Ceramic Society 16 (1996) 703–713

0955-2219(95)00199-9
0955-2219/96/$15.00

Mechanical Behaviour of Silicon–Silicon Carbide Composites

E. Scafè,[a] G. Giunta,[a] L. Fabbri,[a]* L. Di Rese,[a] G. De Portu[b] & S. Guicciardi[b]

[a]Eniricerche SpA, via E. Ramarini 32, 00016 Monterotondo (Roma), Italy
[b]Istituto di Ricerche Tecnologiche per la Ceramica, CNR, via Granarolo 64, 48018 Faenza (Ravenna), Italy

(Received 5 September 1994; revised version received 24 October 1995; accepted 1 November 1995)

Abstract

The dependence on the composition of Young's modulus, fracture toughness and flexural strength of a reaction-sintered (RS) silicon–silicon carbide (Si–SiC) composite was determined at room temperature over a wide range of SiC content (0–90 vol%). The results were compared with those of two commercial reaction-bonded (RB) Si–SiC materials. Young's modulus follows two-phase models over the whole compositional range when a value of 432 GPa is assumed for the Young's modulus of β-SiC. At low SiC contents (<60 vol%), the RS composites show fracture behaviour consistent with a crack-deflection toughening model, while at SiC content higher than about 70 vol%, they exhibit much higher surface energies than the equivalent RB commercial Si–SiC. Between 60 and 70 vol% SiC an abrupt change of fracture behaviour is observed. Such differences in surface energies are attributed to quite different microstructures and crack propagation mechanisms.

1 Introduction

In the late 1970s, researchers at General Electric proposed a new way to prepare silicon carbide-based ceramics;[1] they succeeded in obtaining a reaction-sintered (RS) Si–SiC material (Silcomp®) from the reaction between liquid silicon and aligned carbon fibres without the addition of silicon carbide powder. At Eniricerche an alternative method for preparing a fully dense, reaction-sintered Si–SiC composite (ER RS) was developed,[2] by direct reaction between silicon and carbon powders.

Both these preparation procedures allowed the almost continuous variation of SiC volume fraction, and each phase was continuous and interpenetrating through the microstructure.[3] The main differences between the materials obtained by the two methods were in the microstructure: the Silcomp® had an aligned SiC fibre in a silicon matrix structure, whereas the ER RS composite was formed by a sponge-like structure of the silicon carbide reinforcement filled with silicon. In the first material some residual unreacted carbon and porosity were present (about 5 vol%), while the second resulted in an almost dense and carbon-free material (≤ 0·5 vol%). Due to its very low porosity, the latter material represents a model suitable for studying the influence of microstructure on mechanical properties. At low SiC content it will be shown that the composite behaves like a brittle matrix with rigid inclusions. At high SiC content it approaches a fully dense polycrystalline β-SiC with some silicon regions acting as defects. In the intermediate region an abrupt change in the fracture behaviour is observed.

In order to better understand the microstructure–properties relationships of these composites at high SiC contents, two well-known materials, Refel[4] and Sigri,[5] were also evaluated and compared with the ER materials. These commercial materials can also be defined as 'interpenetrating phase composites',[3] due to their microstructure and preparation procedure (i.e. silicon infiltration), even though the high SiC content could have broken down the interconnectivity of the silicon phase. As, in general, very different features are reported for Si–SiC materials which have quite similar chemical composition, it will be shown that, as expected, the microstructure has a strong influence on the fracture properties; at the same time however, it does not affect the elastic properties, which follow the two-phase models. In particular, the high SiC content ER RS composites are characterized by the highest value of fracture toughness reported to date for this class of materials. In a previous study,[6] it was proposed that such a feature could be attributed to the different crystalline phases (α- and β-SiC). Now, further microstructural

*Present address: JRC, Ispra (VA), Italy.

investigations, with particular SEM operating conditions, allow us to consider the observed fracture toughness values as primarily being due to other microstructural features.

2 Experimental

A group of RS Si–SiC composites (ER RS-1...8) was prepared in the Eniricerche laboratories. Their properties were analysed and compared with those of three Si–SiC composites: two commercial reaction-bonded materials (rectangular plates, Sigri* 5 × 50 × 50 mm and Refel† type 5 × 50 × 150 mm), and one RS Si–SiC (Silcomp®, literature data only).

The ER RS Si–SiC composites were made by using silicon and carbon powders. The powders were prepared by ball-milling (agate jar) high purity feed-stock materials. Silicon was obtained from a single crystal electronic-grade ingot (B-doped, 1–10 ppma). The impurity content of carbon was of the order of 0·3 wt% (mainly Ca, Al, Fe oxides). After milling, the size distributions of silicon and carbon powders were both below 25 μm with average particle sizes of ~5 μm, as measured by laser scattering method. The SiC content in the final composite material was controlled by varying the relative amount of silicon and carbon powders. These powders were dry-ball mixed and die-pressed (200 MPa) to their final shape (i.e. plates 4 × 10 × 50 mm). The reaction sintering was carried out under vacuum ($\leq 10^{-2}$ Pa), at temperatures higher than the silicon melting point (1450–1700°C). The resulting sponge-like SiC structure was filled with a suitable amount of liquid silicon. The cooling cycle was performed in order to control the volume expansion of silicon (~9%) during solidification. The sintered components did not show any shrinkage for high SiC content (>50 vol%), according to published data on similar materials.[1,4] SIMS–AES analyses[7] on the sintered ER RS Si–SiC materials show ~0·2 at% of Al, due to a contamination from the furnace.

To evaluate phase composition and texture, X-ray powder diffraction was carried out using Cu K_α radiation and a graphite monochromator (Philips, APD 1700).

Microstructural analysis was performed using a Cambridge Stereoscan 360 scanning electron microscope, employing both the backscattering and the secondary mode. The instrument was equipped with a high brightness gun (LaB_6 cathode) and a solid-state backscattered electron detector having high collection efficiency and operating with beam energy ranging between 6 and 30 keV.

To obtain the crystallographic features of grains (down to ~0·5 μm), the electron channelling pattern (ECP) technique was used at low beam energy (6–8 keV).[8,9] ECP conditions were verified by observing the contrasting changes of the polished surface at different orientation angles, relative to the beam, according to the literature.[10]

The volume fractions of each phase (Si, SiC, C and porosity) were determined using image analysis (IA) by sampling at least 50 random regions on samples polished down to 1 μm diamond paste, at 1000× magnification corresponding to an area of 100 × 150 μm. Measurements were taken with a metallographic optical microscope connected to a Quantimet 970. IA was used in order to determine the size distribution of the minority phase regions. Density was obtained by the Archimedes' method according to ASTM C693-84.[11]

Young's modulus was measured by an improved flexural resonance method, described elsewhere,[12,13] based on electrostatic excitation and a laser modulation technique for detecting vibration amplitude. Three different compositions of ER RS Si–SiC (30, 50, 70 vol% SiC) were prepared to select the most appropriate two-phase model, which was used to calculate all Young's modulus values necessary to evaluate the fracture energy γ. Due to the sample thickness (4 × 10 × 50 mm), its effect on the shear modulus was corrected following the ASTM suggestions;[14] three polycrystalline silicon samples, with different thicknesses, were measured in order to check the effectiveness of Pickett's correction term.[15] The reproducibility of the method of Young's modulus determination was of the order of 0·01%; the absolute accuracy was limited by the accuracy of the dimensional measurements. By using adequate machining and measuring procedures, an absolute accuracy better than 1% was obtained.[12,13] In addition, sound velocities (longitudinal and transversal) of some selected samples (50 and 70 vol% SiC) were measured by using an automated cross-correlation method.[16] Ultrasonic measurements were carried out with a buffer rod, while the centre frequencies of the transducers were 10 and 5 MHz for longitudinal and transversal velocity, respectively. The time-domain cross-correlation function of the selected echoes allows the time-of-flight measurements with an uncertainty of ±2 ns. Young's modulus and Poisson's ratio were calculated by the equations reported elsewhere.[16] The ultrasonic data agreed quite well with those measured by flexural resonance on the same samples (Table 2), whereas our values, measured with both methods on commercial RB Si–SiC,

*Silit-SK 308, trade mark for Sigri Elektrographit GmbH, was purchased by 'Elettrocarbonium', Milano, Italy.
†Refel RB Si–SiC, trade mark for UKAEA material, was purchased by TenMat Ltd, Manchester, UK.

were slightly lower in the case of Refel and higher in the case of Sigri (Table 2), than those reported in the literature.[4,5,17–19]

For mechanical testing, samples were machined in order to obtain test-bars (4 × 4 × 40 mm). The surface in tension was polished down to 9 μm grit and the edges were rounded to avoid stress concentration. Three-point flexural strength was measured over a 35 mm span using an Instron 1195 universal testing machine with a crosshead speed of 0·5 mm min^{-1}.

Fracture toughness values were obtained by the single edge notched beam (SENB) technique. The samples (4 × 4 × 20 mm) were carefully notched with a 0·10 mm diamond saw down to one-third of their thickness. They were then broken in three-point bending over a 16 mm span with a crosshead speed of 0·5 mm min^{-1}. The agreement between our experimental values for Sigri and Refel and those previously reported in the literature[5,17–19] on commercial Si–SiC composites was quite good.

The density and Young's modulus values represent the average of at least three samples. Toughness data were averaged on four specimens while, for strength determinations, more than six test-bars were used for each point. Matrix properties were measured on commercial polycrystalline silicon (purchased from Dynamit Nobel Silicon).

3 Results and Discussion

3.1 Microstructure

X-ray diffraction analyses of RB Si–SiC show, as reported in the literature,[20] the presence of the different α (hexagonal) and β (cubic) SiC polytypes, with some texturing effect. The exothermicity of the reaction between silicon and carbon results in a large increase in temperature. A local temperature rise in excess of 400°C, in addition to the operating temperature (1600–1700°C), has been reported for Refel RB Si–SiC.[4] Since, in the RS process, silicon and carbon powders are not diluted by the presence of α-SiC particles, the reaction front temperature is expected to be higher than in the corresponding RB case, approaching the self-propagating reaction regime.[21] In this case, a temperature higher than 2000°C should be attained. As a result, a fraction of an α polytype was expected in the RS composites, as reported in the literature for similar experimental conditions.[22] By contrast, we have observed only the β-SiC polytype in our RS material.

For the two commercial RB composites, quite different microstructures were observed. Refel material shows an enhanced bimodal SiC grain size distribution and exhibits silicon regions with an average diameter of ~11 μm [Figs 1(a) and (b)]. In agreement with the literature data,[20] metallic inclusions (Al, Fe, Ni) and some residual carbon were also observed.[7] Sigri material [Figs 2(a) and (b)] shows much coarser SiC grain size and less enhanced bimodal distribution. Larger silicon regions, with an average diameter of ~17 μm, and metallic inclusions (mainly Al) were also found.

Typical microstructures of ER RS composites show polycrystalline continuous SiC and Si phases belonging to the interpenetrating-type class, that, according to Schulz,[23] can be described as being formed by infinitely long cylinders. ER RS materials exhibit two different morphologies at low (<60 vol%) and high (>70 vol%) SiC content. At low concentrations, large textured silicon regions are found and the SiC polycrystalline regions (Fig. 3) have an average diameter that ranges from 10 to 18 μm as the SiC content varies from 50 to 35 vol% (Figs 4 and 5) respectively. At high SiC concentration, large silicon carbide regions are found, with average silicon domains of ~11 μm [Figs 6(a) and (b)], and some residual carbon. The SiC microstructure maintains the sponge-like polycrystalline morphology, with reduced crystalline domains size

(a)

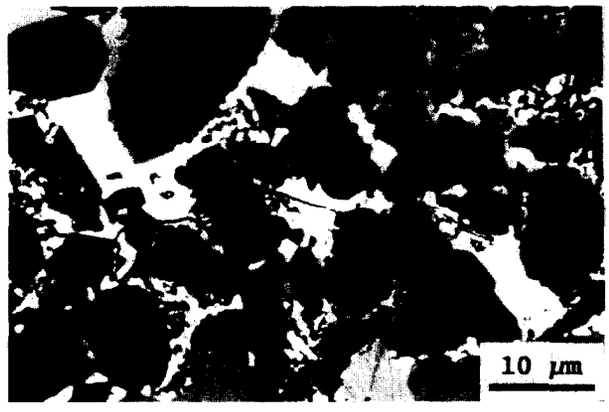

(b)

Fig. 1. (a) Backscattered SEM micrographs of commercial RB Si–SiC composites (Refel material); nearly transgranular fracture is observed. Silicon (grey regions), silicon carbide (89 vol%) (dark regions), carbon (black regions), metallic inclusions (white regions); phase morphology is similar to those reported in the literature.[20] (b) As (a) but using ECP technique.

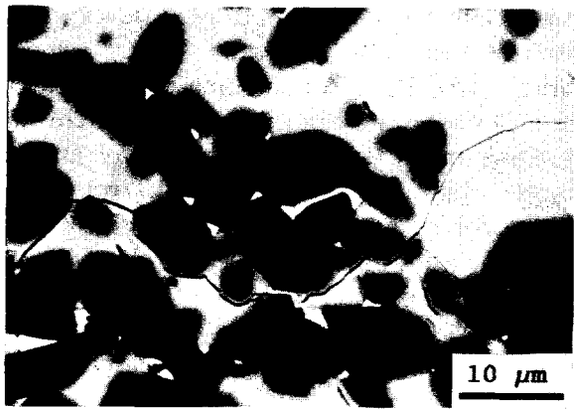

(a)

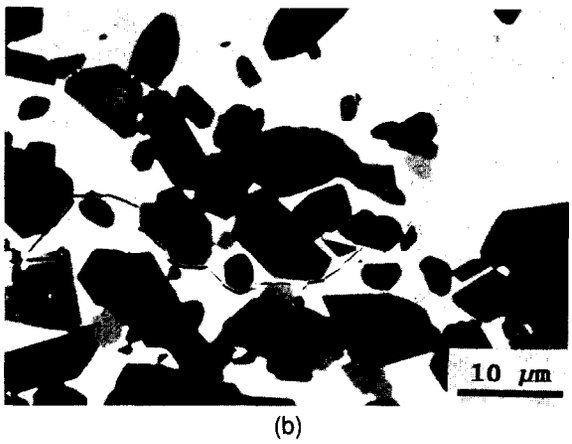

(b)

Fig. 2. (a) Backscattered SEM micrographs of commercial RB Si–SiC composites (Sigri): silicon carbide (82 vol%). Crack deflection is evidently operating. (b) As (a) but using ECP conditions.

Fig. 3. Backscattered SEM ECP micrograph of ER RS Si–SiC composites: silicon and polycrystalline silicon carbide (35 vol%). SiC grain exhibits different orientations.

(Fig. 7) containing a high density of twins. SiC grains did not show crystallographic texture effects.

The total amount of residual unreacted carbon and porosity (V_{ext}), measured by using IA, was generally less than 0·5 vol% (Table 1); these values were lower than those reported in the literature for the Silcomp® material.[24] The SiC volume fraction values used for the analysis of material properties were calculated using the 'rule of mixtures' and the experimental density data as measured by Archimedes' method, considering 2·33 and 3·21 g cm^{-3}

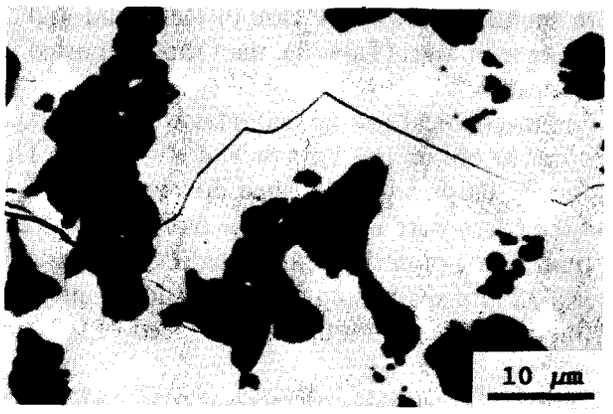

Fig. 4. Backscattered SEM micrograph of ER RS Si–SiC composites; polycrystalline silicon carbide (35 vol%). Crack moves mainly in silicon region and is deflected by SiC grains.

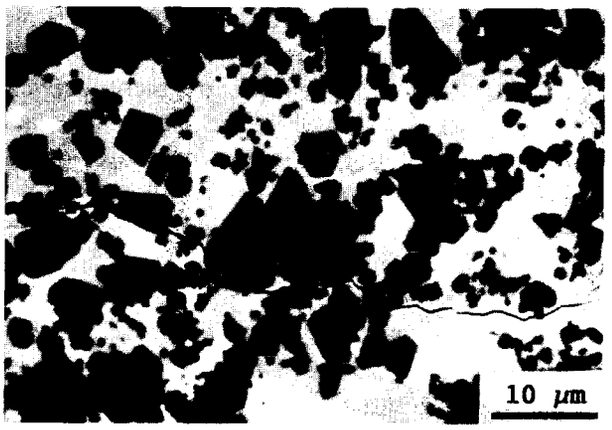

Fig. 5. Backscattered SEM micrographs of ER RS Si–SiC composites; polycrystalline silicon carbide (50 vol%). Also, at this SiC content, the crack moves mainly in the silicon region and is deflected by SiC grains.

as the density of Si and SiC respectively. The comparison between density data and density values, calculated using the same procedure, and the volume fractions obtained by IA, leads to reasonable agreement due to the low values of unreacted carbon and porosity (Table 1 and Fig. 8).

3.2 Elastic properties

The experimental data obtained on Si–SiC materials were compared with the values obtained from the composite theory. Among the different two-phase models available in the literature, the near fully dense Si–SiC composites follow quite well the absolute bounds models as already reported.[12,25] In particular, because more stringent hypotheses about the microstructure of the composite could be formulated, such as an isotropic and quasi-homogeneous distribution of phases, a more accurate model having narrower limits may be applicable: the Hashin–Shtrikman (HS) model.[26] Homogeneous phase distributions were observed for all Si–SiC composites. In this case the HS model could be applied once the elastic properties of the phases were known. The theoretical upper limits

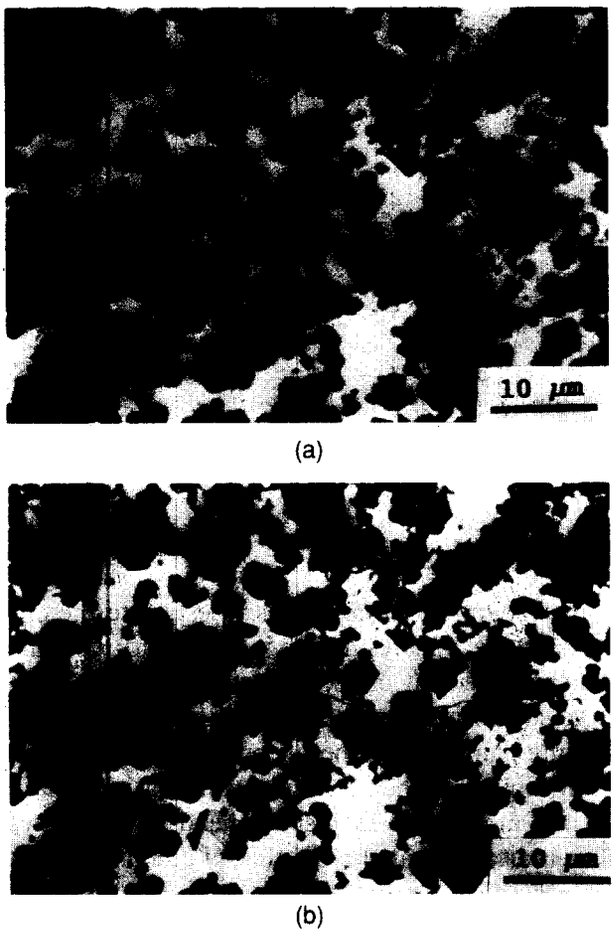

Fig. 6. (a) Backscattered SEM micrographs of ER RS Si–SiC composites: sponge-like polycrystalline SiC morphology (70 vol%) (dark regions); residual carbon (black regions). The crack passes mainly in the polycrystalline SiC regions. (b) As (a) but using ECP technique.

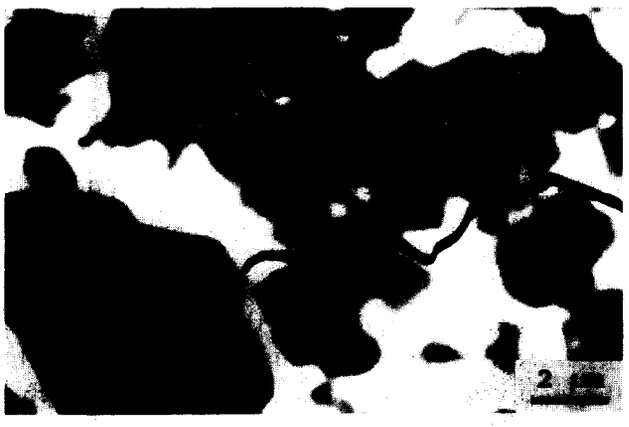

Fig. 7. SEM backscattered ECP micrograph at high magnification of ER RS Si-SiC composite: the crack is also deflected inside the SiC grain (dark region) according to its polycrystalline structure.

for bulk (K_u) and shear moduli (G_u) can be calculated by the following relationships:[26]

$$K_u = K_2 + \frac{V_1}{1/(K_1 - K_2) + 3V_2/(3K_2 + 4G_2)} \quad (1)$$

$$G_u = G_2 + \frac{V_1}{1/(G_1 - G_2) + 6V_2\,(K_2 + G_2)/5G_2(3K_2 + 4G_2)} \quad (2)$$

where V, K and G are volume fraction, bulk modulus and shear modulus, respectively, and the subscripts 1 and 2 refer to Si and SiC phases, respectively. The lower limits (K_1, G_1) are obtained from the previous equations by interchanging the indices 1 and 2.

In order to compare our experimental data with the predicted elastic properties, the upper bounds to Young's modulus (E_u) and Poisson's ratio (ν_u) were calculated by the following relationships:

$$E_u = 9K_uG_u/(3K_u + G_u) \quad \nu_u = (3K_u - 2G_u)/(6K_u + 2G_u) \quad (3)$$

The lower limits (E_1, ν_1) were calculated by interchanging the indices u with 1.

Due to the availability of high-quality large silicon single crystals, very accurate values of the elastic constants, measured by acoustical methods, are reported in the literature.[27] By using these data, in addition to the averaging procedure due to Voigt, Reuss and Hill,[25] the calculated Young's modulus of silicon (E_{ref} in Table 2) was 164 GPa. The calculated average Poisson's ratio, obtained by using the same procedure, was 0·22. Our experimental results on reference samples of polycrystalline silicon are in quite reasonable agreement (168 ± 2 GPa).

Reliable data for elastic constants of SiC single crystals are lacking due to the difficulties in obtaining single crystals large enough to perform accurate acoustic measurements.[28,29] Therefore the elastic properties of polycrystalline β-SiC were derived by using a non-linear least-squares analysis of the whole set of our experimental values. The result was E_{ref} = 432 GPa (Fig. 9). This value is one of the few data reported to date on polycrystalline β-SiC, and can be compared only with the results of theoretical calculations, e.g. 496 GPa[29] or 402 GPa.[30] The experimental values reported in the literature are measured either on whiskers or on α-SiC polytypic, polycrystalline ceramic samples, resulting in 436 GPa[31] and 448 GPa,[23] respectively.

By using these values (168 and 432 GPa for Si and SiC phases, respectively) the commercial RB Si–SiC composites can also be fitted to the same theoretical model, even though there is a mixture of α–SiC and β–SiC polytypes.

3.3 Mechanical properties

As mentioned above, Figs 11 and 12 illustrate the complex behaviour of fracture toughness and strength as a function of SiC content. Two different regions are clearly identifiable, below and above the value of about 65 ± 5 vol% SiC, which is inferred from our experimental points that are at 59 and 69 vol% SiC. The value 65 ± 5 vol% SiC could be regarded as a sort of percolation threshold for silicon in the SiC matrix.

Table 1. Microstructural characteristics of Si–SiC composites. ρ_{calcul} represents the bulk density as measured by using image analysis data

Sample	*Grain size* (μm)	ρ_{exp} ($g\ cm^{-3}$)	V_{SiC} (*vol%*)	V_{Si} (*vol%*)	V_{ext} (*vol%*)	ρ_{calcul} ($g\ cm^{-3}$)
Poly-Si	100	2·33	0	100	0	2·33
Sigri	17[a]	3·051	82·4	17·4	0·2	3·050
Refel	11[a]	3·110	84·6	15·3	0·1	3·072
ER RS-1	n.m.	2·612	32·8	67	0·2	2·614
ER RS-2	18[b]	2·642	35·4	64·4	0·2	2·637
ER RS-3	n.m.	2·674	37·2	62·5	0·3	2·650
ER RS-4	n.m.	2·735	46·5	53	0·5	2·728
ER RS-5	10[b]	2·779	51·4	48·4	0·2	2·778
ER RS-6	n.m.	2·845	59·1	40·7	0·2	2·845
ER RS-7	11[a]	2·923	68·9	30·6	0·5	2·925
ER RS-8	n.m.	3·101	87	12	1·0	3·072

[a]Silicon region.
[b]Silicon carbide regions.
n.m.: not measured.

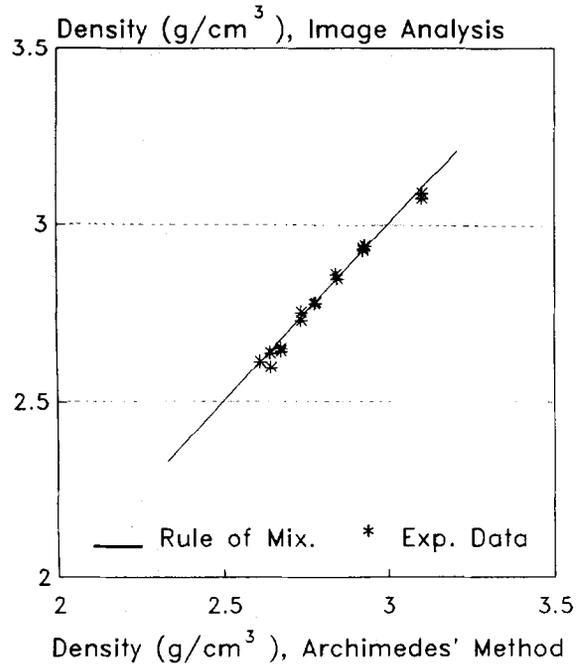

Fig. 8. Experimental values of density measured by the Archimedes' method (*x*-axis) vs. values obtained by image analysis (*y*-axis).

For SiC content between 0 and 60 vol%, the ER RS Si–SiC composites behave like the particulate composites described in the literature by Faber and Evans (FE):[33] the toughness increases rapidly at the first introduction of the reinforcement, and slowly thereafter (Fig. 11). At low SiC content, the fracture toughness values of ER RS material agree quite well with those reported for Silcomp® (longitudinal direction[24]) even though the two RS composites, which contain β-SiC crystals in both cases, have quite different morphologies: Silcomp® exhibits longitudinally aligned grains up to 50 μm in size[24] and the ER composite has a sponge-like microstructure with 2 μm grains.

To identify toughness mechanisms, stable cracks were produced by indentation (Knoop indenter, with a load of 20 N) of the polished surfaces of both RB and RS composites to estimate the crack front profile. Figures 4 and 5, relative to RS materials, show evident crack deflection examples inside large silicon regions. Apart from hypothetical weak fracture planes inside the silicon region, this phenomenon happens when a crack, running in a matrix, finds a more rigid inclusion ahead and deviates.[34] This indicates that the FE theory could be applied. To utilize FE results, the shape of the reinforcing phase has to be determined. Due to the interpenetrating-type microstructure, the second phase can be described as being formed by infinitely long cylinders; therefore the aspect ratio value is taken as equal to 12.[33] For these concentrations the experimental values of fracture toughness, K_{exp}, were compared with those calculated according to FE theory:

$$K_{th} = A\,(2\gamma_{Si}E_c)^{1/2} \qquad (4)$$

where A, which depends on the aspect ratio of the second phase, was assumed to be equal to 2;[33] γ_{Si} is the silicon matrix fracture energy (2.7 J m^{-2}, Ref. 35); and E_c is the Young's modulus of the composite calculated using the HS model, which fits our experimental results. Table 3 shows that the agreement can be considered very satisfactory and could justify a posteriori the assumed crack-deflection toughening mechanism for these composites at low SiC content.

In the neighbourhood of 65 vol% SiC, an abrupt change in fracture toughness of the ER RS composites is observed. A possible explanation could be attributed to the fact that at this SiC content the interconnectivity of the silicon region may have broken down to give discrete silicon particles[3] which act mainly as defects. This fact is consistent with the different behaviour of the other RS composite (Silcomp®), which is reinforced with fibres. Concerning RB commercial materials, we did not find any data about composites with low SiC

Table 2. Elastic properties of Si–SiC composites obtained by using different techniques (ultrasonic and resonance methods). Numbers within brackets represent the experimental errors

Specimen	*Thickness (mm)*	V_{SiC} *(vol%)*	E_{reson} *(GPa)*	E_{ultras} *(GPa)*	ν	E_{ref} *(GPa)*
Poly-Si-1	2·06	0	168 (2)			164[e]
Poly-Si-2	3·01	0	168 (2)			164[e]
Poly-Si-3	3·48	0	167 (2)			164[e]
Sigri	3·98	82[a]	375 (4)	371 (3)	0·17	375[e]
Sigri		82[b]				310[b]
Refel	3·97	89[a]	382 (4)	387 (3)	0·17	386[e]
Refel		90[c]				409[c]
ER RS-2		35[a]	234 (4)			230[e]
ER RS-5		51[a]	258 (2)	260 (3)	0·20	260[e]
ER RS-7		68[a]	322 (4)	323 (3)	0·19	320[e]
Silcomp-1		20–25[d]				200[d]
Silcomp-2		40–45[d]				303[d]
Silcomp-3		80–85[d]				350[d]

[a]Averaged on four samples.
[b]Literature data.[5]
[c]Literature data.[18,19]
[d]Literature data.[24]
[e]Calculated from theory.

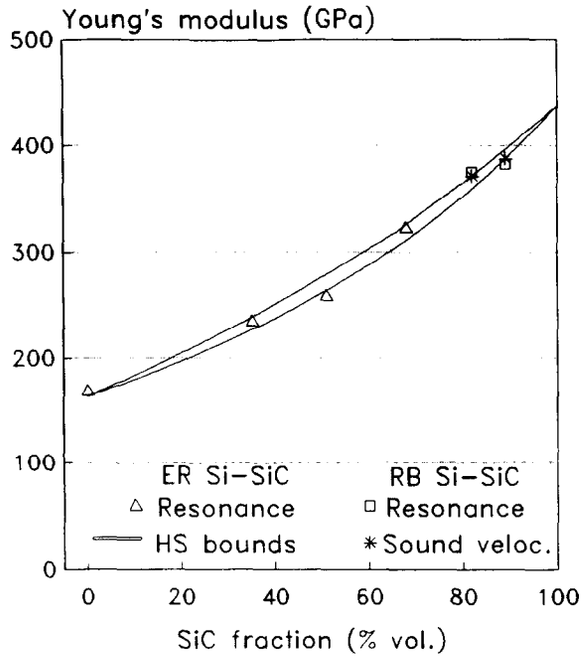

Fig. 9. Experimental values of Young's modulus vs. SiC volume fraction. Solid lines represent the Hashin–Shtrikman bounds.

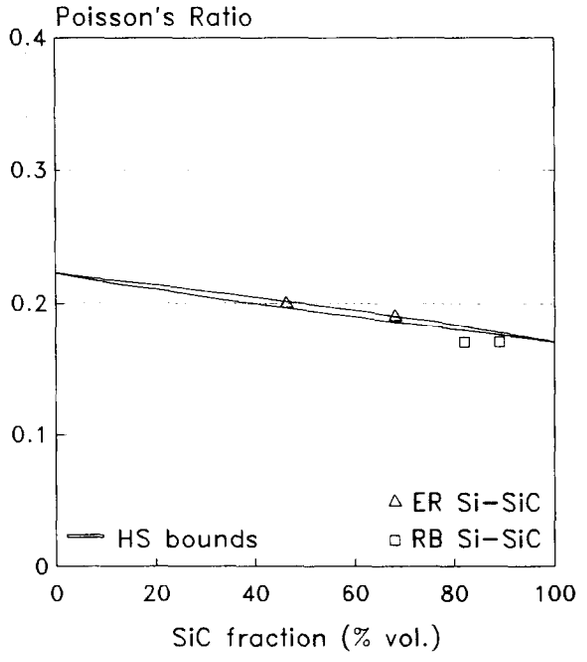

Fig. 10. Experimental values of Poisson's ratio vs. SiC volume fraction. Solid lines represent the Hashin–Shtrikman bounds.

content; some Refel materials were studied as a function of composition[19] but the SiC content was in the range 75–95 vol%, well above the supposed percolation threshold of silicon. From this point of view, the properties of RB commercial materials should be compared with those of the RS composites in the range >65 vol% SiC.

At SiC content >65 vol%, the two composites (ER RS-7 and ER RS-8) show a slight increase in fracture toughness which probably is associated with the similar increase in Young's modulus. The comparison between the RB and RS composites, at similar SiC volume fraction, shows a much tougher behaviour of RS Si–SiC materials. In particular, the γ values of ER RS-7 and ER RS-8 composites, calculated from $\gamma = K_{IC}^2/(2E)$, are higher than the value of 30 J m^{-2} reported in the literature for SiC ceramics,[36] and are also considerably higher than the corresponding values calculated for the RB Si–SiC commercial materials which, for the Refel composite (Table 3), agree reasonably with those already published.[18,19]

It is reported in the literature that interpenetrating-phase composites could benefit from further toughening mechanisms such as crack-bridging,[3,37,38] therefore the load–displacement curves and the corresponding micrographs were carefully examined. In all the tests the load–displacement curves did not show any curvature before fracture, indicating no evidence of *R*-curve in these materials.[37,38] The

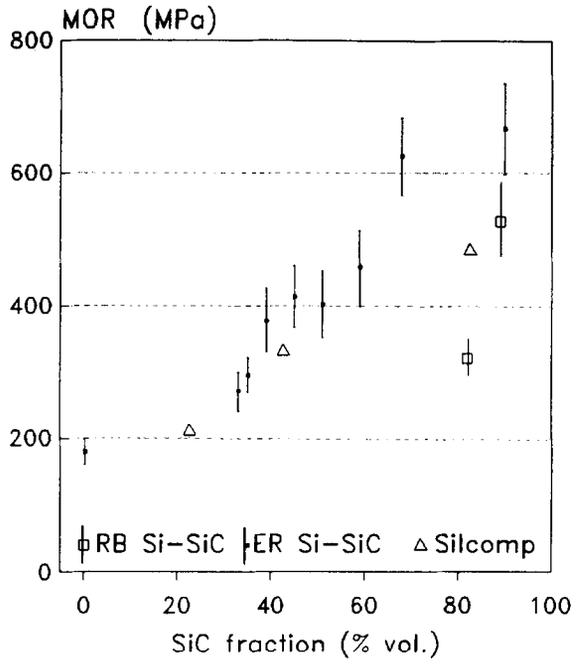

Fig. 11. Experimental values of flexural strength vs. SiC volume fraction.

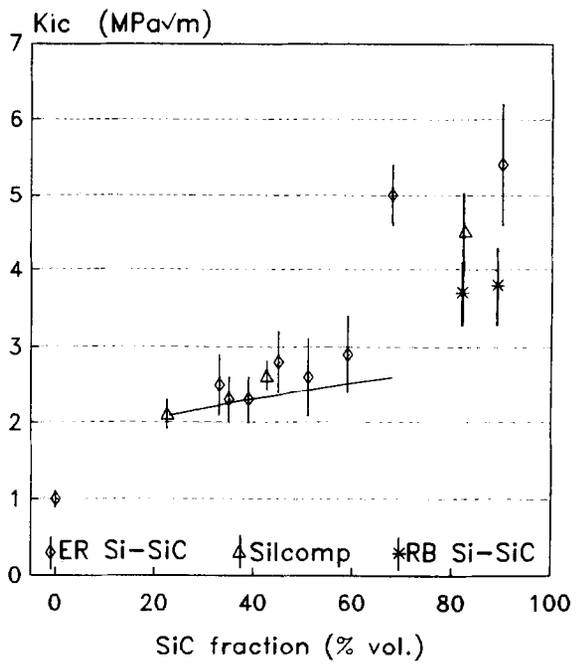

Fig. 12. Experimental values of fracture toughness by SENB method of different Si–SiC composites. Solid line shows the behaviour according to the Faber–Evans crack-deflection theory.

Table 3. Mechanical properties of Si–SiC composites. Numbers within brackets represent the experimental errors

Specimen	V_{SiC}[c] *(vol%)*	E_{calc}[d] *(GPa)*	ν_{calc}[d]	K_{IC} *(MPa m$^{1/2}$)*	K_{th}[e] *(MPa m$^{1/2}$)*	σ *(MPa)*	c *(μm)*	γ *(J m^{-2})*
Poly-Si	0	164	0·22	1·0 (0·1)	–	180 (20)	20	2·7
ER RS-1	33	226	0·20	2·5 (0·4)	2·2	270 (30)	56	13·0
ER RS-2	35	230	0·20	2·3 (0·3)	2·2	295 (27)	40	11·0
ER RS-3	39	239	0·20	2·3 (0·3)	2·3	378 (30)	24	10·0
ER RS-4	45	253	0·20	2·8 (0·4)	2·3	413 (46)	30	12·0
ER RS-5	51	268	0·19	2·6 (0·5)	2·4	402 (50)	27	12·0
ER RS-6	59	289	0·19	2·9 (0·5)	2·5	456 (56)	26	14·0
ER RS-7	68	316	0·18	5·0 (0·4)	–	625 (59)	42	38·0
ER RS-8	90	390	0·17	5·4 (0·8)	–	667 (69)	43	38·0
Sigri	82	–	–	3·7 (0·4)	–	320 (30)	87	18·0
Refel	89	–	–	3·8 (0·5)	–	525 (60)	34	19·0
Refel[a]	90	–	–	3·4	–	539	26	14·0
Silcomp-1[b]	20–25	–	–	2·1 (0·2)	–	210 (20)	65	11·0
Silcomp-2[b]	40–45	–	–	2·6 (0·2)	–	331 (20)	41	11·0
Silcomp-3[b]	80–85	–	–	4·5 (0·5)	–	483 (50)	57	29·0

[a]Literature data.[18]
[b]Literature data.[23]
[c]Averaged on eight samples.
[d]Calculated with the HS two-phase model.
[e]Calculated with the Faber–Evans model.

sudden load drop at fracture could also have been caused by too large a notch width but, as can be seen on the crack micrographs, behind the crack tip we did not find any indication of the main mechanism of *R*-curve in ceramics, i.e. crack bridging.[37] Moreover, the fracture toughness, as measured by SENB, is representative of the material as a whole and not of any specific individual phase: such fracture toughness values have to be considered relative to a crack that sees the microstructure around it as a homogeneous medium.

The overall fracture energy of these classes of composites can be described as the combination of two main mechanisms. The first one is related to the low/high fracture energy regions (i.e. Si and SiC and Si–SiC interface) intersected by the crack. The second one is the energy absorbed by any other toughening mechanism, such as crack deflection. Stable cracks, such as those introduced by indentation, have been reported to preferentially follow low energy paths in monolithic ceramics.[39–40] By the same principle, therefore, they should allow the features indicative of the crack propagation path between the different phases in our materials to be revealed. Moreover, by this technique, one should be able to ascertain

if the Si–SiC interface is the basic strength-controlling factor of these materials, as already reported.[20]

In the Sigri composite, the crack appears to move preferentially at Si–SiC interface or, at least, quite close to it (Fig. 2). In the Refel composite, the crack crosses both phases with a straighter path (Fig. 1); the crack follows the Si–SiC interface much less than in Sigri material, if at all. The single-crystal SiC grains appear to be cleaved. The similar experimental values of fracture toughness in both RB composites seem to indicate that the fracture of Si and SiC regions and crack deflection lead to the same balance for the overall fracture toughness of this type of composite.

In the ER RS composites, the crack profile crosses both phases and apparently in a way similar to that of Refel material [Figs 6(a) and (b)], with some occasional crack branching. Again, no evidence of a weak Si–SiC interface is found. But SEM micrographs of ER RS composites, at higher magnification (Fig.7) and in ECP conditions, show that the crack was also deflected inside the SiC grains, because of their polycrystalline structure. In a previous work[6] we proposed that such differences in surface energy were attributable mainly to the different amounts of the cubic and hexagonal crystalline SiC phases present in the RB and RS classes of composites. Now, more accurate SEM analyses enable us to attribute such differences to the quite different microstructures of the materials. In fact, the SiC regions intersected by the crack in the Refel composite [Fig. 1(a)] were mainly rounded single crystals, as detected by ECP [Fig. 1(b)], while in the ER composite complex-shaped polycrystalline SiC regions were observed [Fig. 6(b)]. The more complicated fracture process of polycrystals could account for the higher fracture energies calculated for RS composites than for RB commercial materials.[41] Unbroken SiC or Si grains were never observed behind the crack tip.

From all the facts presented above, we argue that the Si–SiC interface is not the determining factor for the fracture properties of this class of composite. If this were the case, it would not be possible to explain the decisive difference in fracture toughness between Sigri, Refel, Silcomp® and ER RS composites with nearly the same SiC content (see Table 3). Moreover, in the case of ER RS composites, if the Si–SiC interface were the controlling parameter then the γ values would have to remain almost constant for the entire compositional range investigated. The very large values of γ for SiC contents higher than 65 vol% and the fractographic evidence indicate that other microstructural features are responsible for the fracture properties.

The flexural strength of the ER composites shows the same trend as their fracture toughness, with an initial increase followed by a sort of plateau between 40 and 60 vol% SiC (Fig. 12). At lower SiC content (33–35 vol%) the strength values were slightly lower than those expected from toughness data. For SiC content higher than 65 vol%, the flexural strength jumps to higher values. In this region, as reported also for Refel material,[19] the flexural strength increases as silicon content decreases. On this subject, it is noteworthy that our experimental values on Refel material agree well with those reported in the literature over many years and from different sources, thus demonstrating the high reproducibility of the preparation procedure. At the maximum SiC content, the ER composite exhibits the highest values of flexural strength, followed by Refel, Silcomp® and Sigri, respectively.

The critical flaw size (c) of the composites was roughly estimated by $c = (YK_{IC}/\sigma)^2/\pi$, where Y is the shape factor, taken as 1·43 for a surface penny-shaped crack,[42] and K_{IC} is the experimental value measured by the SENB technique. It is very likely that in these materials, at the very first loading, the crack tends to grow inside the silicon regions, which have lower toughness, and then spreads catastrophically into the rest of the material. By using the macroscopic K_{IC}, we intended to estimate the critical flaw size just before the sudden failure. From Table 3, one can see that the critical flaw size is almost the same for ER, Refel and Silcomp®, while Sigri shows larger calculated values. The critical flaw size of ER composites ranges between 24 and 56 μm for all the composition ratios. For the composites with high SiC content, these dimensions match reasonably with the silicon regions present in the microstructure. Some fractographic investigations on broken test-bars indicated silicon-rich regions as effective fracture origins. Nevertheless, by considering the wide range of SiC contents investigated, there seems to be only a minor influence on the second phase on this parameter (see Table 3).

4 Conclusions

Si–SiC composites are statistically homogeneous and isotropic materials that do not show interface effects, so that they can be adequately described by the Hashin–Shtrikman two-phase model when 432 GPa is assumed as the Young's modulus of the cubic SiC phase. In the ER RS composites, crack deflection appears to be the dominant fracture toughening mechanism for SiC content up to 65 ± 5 vol%, if rod-shaped particles with high aspect

ratio are assumed as the reinforcing phase. In Sigri material this mechanism still seems to be evident, even though a larger SiC content is present. At high SiC concentration (>65 ± 5 vol%) the fracture toughness of RS composites is higher (especially for the ER composites) than that of corresponding RB materials. It is proposed that such behaviour depends upon SiC phase morphology (polycrystalline grains) in RS Si–SiC. Silicon–silicon carbide interface does not seem to be the determining factor for the mechanical properties.

Acknowledgements

This work was partially supported by the 'Progetto finalizzato Materiali Speciali per Tecnologie Avanzate' of the Consiglio Nazionale delle Ricerche. The authors are grateful to F. Petrucci, V. Adoncecchi and G. Di Passa for their valuable technical assistance, S. Loreti for X-ray diffraction analyses and P. Alessandrini for scanning electron micrographs. We also thank H. Willems and W. Arnold (Fraunhofer Institut for Nondestructive Testing, Saarbrucken, Germany), for fruitful scientific discussion on ultrasonic characterization techniques.

References

1. Hillig, W. B., Mehan, R. L., Morelock, C. R., De Carlo, V. J. & Laskow, W., Silicon/silicon carbide composites. *Am. Ceram. Soc. Bull.*, **54**[12] (1975) 1054–6.
2. Scafè, E., De Rese, L., Petrucci, F., De Portu, G. & Guicciardi, S., Mechanical properties of reaction sintered Si–SiC composites. In *Advanced Structural Inorganic Composites*. ed. P. Vincenzini. Elsevier Science Publishers B.V., Amsterdam, 1991, pp. 269–75.
3. Clarke, D. R., Interpenetrating phase composites. *J. Am. Ceram. Soc.*, **75**[4] (1992) 739–59.
4. Forrest, C. W., Kennedy, P. & Shennan, J. V., The fabrication and properties of self-bonded silicon carbide bodies. In *Special Ceramics*, Vol. 5, ed P. Popper. British Ceramic Research Association, Stoke-on-Trent, 1972, pp. 99–123.
5. Richter, H., Kleer, G., Herder, W. & Röttebacher, R., Comparative study of the strength properties of slip-cast and of extruded silicon-infiltrated SiC. *Mater. Sci. Eng.*, **71** (1985) 203–8.
6. Scafè, E., Giunta, G., Di Rese, L., Petrucci, F., De Portu, G. & Guicciardi, S., Toughening mechanisms in Si–SiC composites. In *Euro-Ceramics II*, Vol. 2, Structural Ceramics and Composites, ed. G. Ziegler and H. Hausner. Deutsche Keramische Gesellschaft e.V., 1991, pp. 1715–20.
7. Scafè, E., Grillo, G., Fabbri, L. & Vittori, V., SIMS–AUGER and thermal conductivity characterization of Si–SiC materials. *Ceram. Eng. Sci. Proc.*, **13**[9–10] (1992) 918–28.
8. Parretta, A., Camanzi, A., Giunta, G. & Mazzarano, A., Morphological aspects of silicon carbide chemically vapour-deposited on graphite. *J. Mater. Sci.*, **26**, (1991) 6057–62.
9. Joy, D. C., Electron channelling patterns. In *Advanced Techniques for Microstructural Characterization*, ed. R. Krishnan, T. R. Anantharaman, C. S. Pande & O. P. Arora. Trans Tech Publications, Switzerland, (1988), Vol. 16, pp. 81–94.
10. Camanzi, A., Giunta, G., Parretta, A. & Vittori, M., Characterization of ceramic coating by channelling effects in scanning electron microscopy. In *Inst. Phys. Conf. Ser. 93*, Vol. 2, ed. P. J. Goodhew & H. G. Dickinson. Institute of Physics, Bristol, 1988, pp. 525–6.
11. Standard test method for density of glass by buoyancy. *ASTM C693-84*, American Society for Testing and Materials, Philadelphia, PA, 1984.
12. Scafè, E., Di Rese, L., Grillo, G. & Petrucci, F., Young's modulus of Si–SiC two-phase particulate composites. In *Advanced Structural Inorganic Composites*, ed. P. Vincenzini. Elsevier Science Publishers B.V., Amsterdam, 1991, pp. 309–15.
13. Scafè, E., Fabbri, L., Grillo, G. & Di Rese, L., Improved technique for Young's modulus determination by flexural resonance. *Ceram. Eng. Sci. Proc.*, **13**[9–10] (1992) 1094–102.
14. Standard test method for Young's modulus, shear modulus, and Poisson's ratio for ceramic whitewares by resonance. *ASTM C848-78, reapproved 1983*, American Society for Testing and Materials, Philadelphia, PA.
15. Pickett, G., Equations for computing elastic constants from flexural and torsional resonant frequencies of vibration of prisms and cylinders. *Proc. Am. Soc. Testing Mater. ASTEA*, **45** (1945), 846–65.
16. Panakkal, J. P., Willems, H. & Arnold, W., Nondestructive evaluation of elastic parameters of sintered iron powder compacts. *J. Mater. Sci.*, **25** (1990) 1397–402.
17. Sigri Elecktrographit GmbH, Technical notes 834 01 20. Germany.
18. McLaren, J. R., Tappin, G. & Davidge, R. W., The relationship between temperature and environment, texture and strength of self-bonded silicon carbide. *Proc. Br. Ceram. Soc.*, **20** (1972) 259–74.
19. Kennedy, P., Effect of microstructural features on the mechanical properties of REFEL self bonded silicon carbide. In *Non-oxide Technical and Engineering Ceramics*, ed. S. Hampshire. Elsevier, Amsterdam, 1986, pp. 301–17.
20. Ness, J. N. & Page, T. F., Microstructural evolution in reaction-bonded silicon carbide. *J. Mater. Sci.*, **21** (1986) 1377–97.
21. Pampuch, R. & Stobierski, L., Solid combustion synthesis of refractory carbides: (a review). *Ceram. Int.*, **17** (1991) 69–77.
22. Yamado, O., Miyamoto, Y. & Koizumi, M., Self-propagating high-temperature synthesis of the SiC. *J. Mater. Res.*, **1**[2] (1986) 275–9.
23. Schulz, B., Thermal conductivity of porous and highly porous materials. *High Temperature–High Pressure*, **13** (1981) 649–60.
24. Mehan, R. L., Effect of SiC content and orientation on the properties of Si–SiC ceramic composites. *J. Mater. Sci.*, **13** (1978) 358–66.
25. Grimvall, G., Thermophysical properties of materials. In *Selected Topics in Solid State Physics*, Vol. XVIII. North-Holland, Amsterdam, 1986, p. 257.
26. Hashin, Z. & Shtrikman, S., A variational approach to the theory of the elastic behaviour of multiphase materials. *J. Mech. Phys. Solids*, **11** (1963) 127–40.
27. McSkimin, H. J. & Andreatch, P. Jr, Elastic moduli of silicon vs. hydrostatic pressure at 25·0 °C and −195·8°C. *J. Appl. Phys.*, **35** (1964) 2161–5.
28. Lambrecht, W. R. L., Segall, B., Methfessel, M. & van Schilfgaarde, M., Calculated elastic constants and deformation potential of cubic SiC. *Phys. Rev. B*, **44** (1991) 3685–94.
29. Fischer, E. S., Manghnani, M. H., Wang, J. F. & Routbort, J. L., Elastic properties of Al_2O_3 and Si_3N_4 matrix composites with SiC whisker reinforcement. *J. Am. Ceram. Soc.*, **75** (1992) 908–14.